Human Pathology (2023) 141, 43–53

Human PATHOLOGY

www.elsevier.com/locate/humpath

Original contribution

Clinicopathological characteristics and molecular analysis of lymphocyte-rich hepatocellular carcinoma☆,☆☆

Kana Tsutsui MD [a], Masamichi Nakayama MD, PhD [a,*], Sachiko Ogasawara PhD [a], Jun Akiba MD, PhD [b], Reiichiro Kondo MD, PhD [a], Yutaro Mihara MD, PhD [a], Yuta Yano MD, PhD [a], Shinji Mizuochi MD, PhD [a], Yoshinao Kinjo MD, PhD [a], Kenta Murotani PhD [c], Hirohisa Yano MD, PhD [a]

[a] *Department of Pathology, Kurume University School of Medicine, Kurume, 830-0011, Japan*
[b] *Department of Diagnostic Pathology, Kurume University Hospital, Kurume, 830-0011, Japan*
[c] *Biostatistics Center, Kurume University, Kurume, 830-0011, Japan*

Received 23 July 2023; revised 8 September 2023; accepted 18 September 2023

Available online 22 September 2023

Keywords:
Hepatocellular carcinoma;
Lymphocyte-rich subtype;
Lymphoepithelioma-like carcinoma;
CCL20;
CCR6

Summary Lymphocyte-rich hepatocellular carcinoma (LR-HCC), a newly proposed subtype of HCC, is characterized with abundant lymphocyte infiltration in the tumor. LR-HCC has a relatively good prognosis and is quite rare (<1% of all HCC). We examined LR-HCC clinicopathological and molecular characteristics by analyzing 451 surgically resected HCC cases without any prior treatment history at our hospital between 2012 and 2021. Clinicopathological features of LR-HCC and other HCCs (non-LR-HCC) were compared. Neoplastic and nonneoplastic hepatocytes from LR-HCC (n = 4) were collected with a laser microdissection system; RNA was extracted, followed by microarray analysis to examine lymphocytic infiltration-related molecular targets. Immunohistochemical staining of identified molecular target was performed in LR-HCC and non-LR-HCC. CD3, CD20, and CD8 immunostaining was also performed in LR-HCCs. There were 28 cases of LR-HCC (6%). No statistically significant differences were found in clinicopathological features, except for gross type, between LR-HCC and non-LR-HCC cases. The LR-HCC 5-year survival rate was >90%. Microarray analysis revealed high CCL20 expression in LR-HCC cases; immunohistochemical study showed significantly higher CCL20 expression in LR-HCC ($P < 0.01$) than in non-LR-HCC. CCR6, the only CCL20 receptor, was observed

☆ Disclosures: None.
☆☆ Funding: This research did not receive any specific grant from funding agencies in the public, commercial, or not-for-profit sectors.
* Corresponding author. Department of Pathology, Kurume University School of Medicine, Asahi-machi 67, Kurume, 830-0011, Japan.
E-mail addresses: tstustui_kana@kurume-u.ac.jp (K. Tsutsui), nakayama_masamichi@kurume-u.ac.jp (M. Nakayama), sachiko@kurume-u.ac.jp (S. Ogasawara), akiba@kurume-u.ac.jp (J. Akiba), kondou_reiichirou@kurume-u.ac.jp (R. Kondo), mihara_yuutarou@kurume-u.ac.jp (Y. Mihara), yano_yuuta@kurume-u.ac.jp (Y. Yano), mizuochi_shinji@med.kurume-u.ac.jp (S. Mizuochi), kinjou_yoshinao@kurume-u.ac.jp (Y. Kinjo), kmurotani@kurume-u.ac.jp (K. Murotani), hiroyano@kurume-u.ac.jp (H. Yano).

https://doi.org/10.1016/j.humpath.2023.09.004

in infiltrating lymphocytes and HCC cells in LR-HCC. There were significantly more CD3-positive cells than CD20-positive cells ($P < 0.0001$) in tumor-infiltrating lymphocytes, most of which were CD8-positive T cells. In conclusion, there were no significant differences in clinicopathological characteristics between LR-HCC and non-LR-HCC, except for gross and LR microscopic features. CCL20 expression in LR-HCC may contribute to infiltration of large numbers of CD8-positive lymphocytes.

1. Introduction

Hepatocellular carcinoma (HCC) is one of the most common cancers worldwide. The prognosis of patients with HCC has been improving over the past decades owing to the screening and early detection of high-risk cases, and the introduction of molecular targeted therapy and immune checkpoint inhibitors. However, it remains the third leading cause of cancer-related death and continues to be associated with poor prognosis [1−3].

HCC with high lymphocytic infiltration was previously classified as lymphoepithelioma-like HCC (LEL-HCC). However, in the 2019 WHO Classification of Digestive System Tumors, 5th Edition, a new designation, "lymphocyte-rich HCC" (LR-HCC), was proposed. LR-HCC is almost never associated with Epstein−Barr virus (EBV), which has been linked to LEL-carcinomas (LELC) in other organs. Its frequency is less than 1% of all HCC cases [1]. A PubMed literature search using the keywords "lymphoepithelioma-like HCC'" and "HCC lymphocyte rich" yielded 66 cases with detailed reports as of 2020 (41 male and 25 female patients; average age, 60.3 years [39−89 years]). Of these 66 cases, 30 were positive (48%) for HBV and 22 were positive (32%) for HCV. Furthermore, compared to conventional HCC, LR-HCC has relatively good prognosis [1,4−17]. Evaluating the clinicopathological characteristics of LR-HCC may help predict the prognosis and elucidate new treatment methods.

Multiple molecular and genomic analyses have been reported for lymphoepithelioma and LELC. EBV infection and carcinogenesis have been analyzed [18], and the genomic analysis of a coherent case of pulmonary LELC has been reported [19]. Ohtani H et al. reported that the CXCL9-CXCR3 axis is involved in the formation of the lymphoid stroma in lymphocyte-rich gastric carcinoma [20]. However, LR-HCC is not associated with EBV infection, and the mechanisms of its development and the molecular targets that contribute to tumor maintenance and promotion are likely to be different. Recently, the genomic structure of HCC has been comprehensively elucidated, and the mechanism of carcinogenesis is being elucidated [21]; nonetheless, the detailed characteristics of LR-HCC are still unclear, because of its rarity and because it is a relatively new subtype.

In this study, we retrospectively evaluated the frequency and clinicopathologic significance of LR-HCC among the resected HCCs at our institution and identified LR-HCC-specific genes by comprehensive microarray analysis, followed by immunohistochemistry to examine the protein expression of key molecular candidates.

2. Materials and methods

2.1. Patients

We evaluated 915 cases of HCC pathologically diagnosed after surgical hepatectomy for primary liver tumors at Kurume University Hospital during the 10-year period from 2012 to 2021. Cases with recurrence, cases treated preoperatively with local therapy (radiofrequency ablation, transcatheter arterial embolization, etc.) or systemic therapy (chemotherapy, molecular targeted drugs, etc.), and cases in which portal vein embolization was performed preoperatively were excluded and consequently, 451 cases were included in the study. This study was approved by the ethical committee of Kurume University (approval no. 22161) and conformed to the 1964 Declaration of Helsinki and its later amendments or comparable ethical standards. An opt-out policy was used in this study.

2.2. Clinicopathological information and follow-up parameters

Clinical data were obtained retrospectively from electronic medical records. This information included patient demographics (sex, age, medical history), clinical staging, and pathology reports. Prognostic metrics, such as overall survival (OS) and recurrence-free survival (RFS), were determined based on outpatient visit history, telephone surveys, clinical examinations, and imaging findings, such as CT scans. This information was used to ascertain the date of death, confirmation of survival, and/or date of recurrence. OS and RFS were then calculated from the number of days after surgery.

2.3. Pathological assessment

Liver specimens were fixed in 10% buffered formalin, followed by paraffin embedding. We cut consecutive 4-μm thick sections and stained them with Hematoxylin and Eosin (H&E). Morphological observations were conducted

in H&E-stained sections under a light microscope (low magnification ×40 to high magnification ×400; CX41; Olympus Corporation, Tokyo, Japan). The histologic diagnosis of HCC was reviewed and confirmed by two pathologists (K.T. and M.N.). Criteria of selection of LR-HCC were derived from a previous report from our institution; specifically, LR-HCC was defined on the observation of >100 tumor-infiltrating lymphocytes under a high-power field (HPF) across ten fields [6]. We compared clinicopathological factors between the extracted LR-HCC and other HCC (non-LR-HCC) groups.

2.4. Laser microdissection (LMD) and total RNA isolation

Four cases were selected for the sample from the LR-HCC cases and these formalin-fixed, paraffin embedded (FFPE) samples were cut to 8-μm sections and stained with 0.05% Toluidine blue after deparaffinization. Neoplastic hepatocytes and paired nonneoplastic hepatocytes, excluding lymphocytes, were microdissected using the LMD system (Leica LMD6000, Leica Microsystems GmbH, Wetzlar, Germany).

The total RNAs in each specimen were extracted using the Qiagen AllPrep DNA/RNA FFPE kit (Qiagen, Hilden, Germany). RNA samples were quantified by an ND-1000 spectrophotometer (NanoDrop Technologies, Wilmington, DE, USA) and the quality was confirmed with the TapeStation system (Agilent technologies, Santa Clara, CA, USA).

2.5. Gene expression microarrays

The cRNA was amplified, labeled with total RNA using GeneChip® WT Pico Kit, and hybridized to Thermo Fisher Scientific Clariom™ D Assay, Human according to the manufacturer's instructions (Thermo Fisher Scientific, Inc., Waltham, MA, USA). All hybridized microarrays were scanned by a Thermo Fisher Scientific scanner. Relative hybridization intensities and background hybridization values were calculated using Expression Console™ (Thermo Fisher Scientific, Inc.).

2.6. Data analysis and filter criteria

The raw signal intensities of all samples were normalized with SST-RMA algorithm (gene level) using Thermo Fisher Scientific Expression Console version 1.4.1 software. To identify up or down-regulated genes, we calculated Z-scores [22] and ratios (non-log scaled fold-change) from the normalized signal intensities of each probe for comparison between control and experiment sample.

Then we established criteria for regulated genes: (up-regulated genes) Z-score $\geq$2.0 and ratio $\geq$1.5-fold, (down-regulated genes) Z-score ≤ -2.0 and ratio $\leq$0.66.

2.7. Immunohistochemistry

To further validate the expression of the candidate gene identified by microarrays at the protein level and their relationships with clinicopathological factors, immunohistochemical (IHC) staining was performed on 4-μm FFPE tissue sections from cases of LR-HCC and HCC without massive lymphocyte infiltration as a control (non-LR-HCC). From the results described below, there were 28 cases of LR-HCC and an equivalent number of 30 cases were selected for the control group. The controls were randomly selected from 432 non-LR-HCC cases and ensured that there was no statistically significant difference in clinicopathological background compared to the population. The molecular target we focused on is CC motif chemokine ligand (CCL) 20. For CCL20 stain, the sections were deparaffinized and rehydrated with xylene and 100% graded ethanol, respectively. The sections were subsequently soaked in Target Retrieval Solution, pH 9 (Dako; Agilent Technologies, Inc., Santa Clara, CA, USA) and treated at 110 °C in a pressure cooker for 15 min. IHC staining was performed using the EnVision system (Dako) according to the manufacturer's protocol and tissue sections were incubated with the primary antibody for overnight at 4 °C. The primary antibody used was a rabbit monoclonal anti-human CCL20 (1:200, #26527-1-AP, Proteintech Group, Inc., Rosemont, IL, USA). In addition, CC motif chemokine receptor (CCR) 6 (rabbit monoclonal, 1:1000, #ab227036, Abcam, Cambridge, UK), the only receptor for CCL20, was stained using the same procedure.

The results of the staining were evaluated independently, according to the staining intensity and the percentage of positive cells, by two pathologists (K.T. and M.N.), using the previously described light microscope. Initially, the whole slide was observed at ×40 magnification in order to assess the percentage of stained area. The staining intensity was then assessed at ×200 magnification. The number of fields of view assessed depended on the stained area percentage. The staining intensity of the cancerous areas was scored on a scale from 0 to 3 compared with the noncancerous area, as follows: 0, when the intensity in the cancerous area was equal to that of the noncancerous area; 1, when the intensity in the cancerous area was slightly higher than that in the noncancerous area; 2, moderately higher and 3, markedly higher. The total expression score in the cancerous area was calculated by multiplying the staining intensity score by the percentage of stained area (Modified Score: MS, range 0−3) [23].

In addition, IHC analysis was performed in FFPE specimens of LR-HCC to evaluate infiltrating lymphocytes using the following antibodies: CD3 (rabbit polyclonal,

Table 1 Clinicopathological factors of the cases of lymphocyte-rich hepatocellular carcinoma and non-LR-HCC.

Clinicopathological factor	LR-HCC (n = 28) (%)	non-LR-HCC (n = 423) (%)	*P*-value
Age, years; mean ± SD	70.3 ± 10.6	70.6 ± 9.5	0.9665
Gender, male/female	23/5 (82.1/17.9)	314/109 (74.2/25.8)	0.5005
Virus infection, HCV/HBV	14/4 (50/14.3)	222/63 (52.5/14.9)	0.7990/0.6447
Gross type			0.0037
Simple nodular type	21 (75)	250 (59.1)	
Simple nodular type with extranodular growth	2 (7.1)	88 (20.8)	
Confluent multinodular type	2 (7.1)	35 (8.3)	
Small nodular type with indistinct margin	2 (7.1)	45 (10.6)	
Unclassified type, Others	1 (3.6)	5 (1.2)	
Tumor size, mm; mean ± SD	28.3 ± 14.0	26.7 ± 19.7	0.2927
Histological grade			0.6355
Well-differentiated	1 (3.6)	46 (10.9)	
Moderately-differentiated	26 (92.9)	328 (77.5)	
Poorly-differentiated	1 (3.6)	49 (11.6)	
Capsule formation	12 (42.9)	240 (56.7)	0.1520
Portal vein invasion	10 (35.7)	196 (46.3)	0.5469
Intrahepatic metastasis	0	36 (8.5)	0.1076
Recurrence	6 (21.4)	179 (42.3)	0.0714
Death	2 (7.1)	98 (23.2)	0.4529

Abbreviations: LR-HCC, lymphocyte rich hepatocellular carcinoma; SD, standard deviation; HCV, hepatitis C virus; HBV, hepatitis B virus.

undiluted, Dako, code IS503), CD20 (mouse monoclonal, undiluted, code N1502, Dako), and CD8 (clone SP57, rabbit monoclonal, undiluted, cat, 790-4460, Ventana, Tucson, AZ, USA). IHC stain was performed using the Ventana Benchmark system (Ventana Automated Systems, Tucson, AZ, USA). The number of positive lymphocytes was counted at high magnification in each field of view, and the average of 10 fields of view was derived.

2.8. Statistical analysis

The presence or absence of statistically significant differences between LR-HCC cases and non-LR-HCC cases with respect to differences in clinicopathological background factors was examined using t-tests and chi-square tests. For evaluation of the prognosis, Kaplan−Meier (K-M) curves were estimated for OS and RFS and compared by log-rank

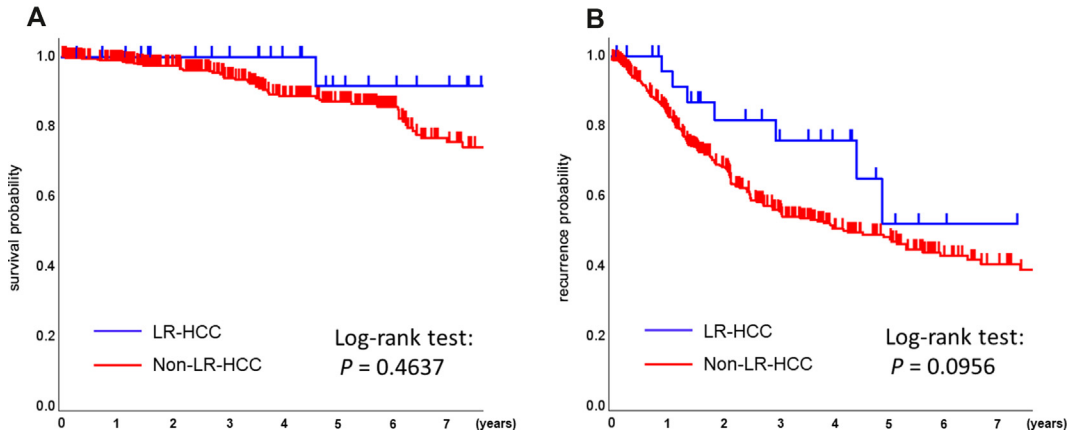

Fig. 1 Overall survival (A) and recurrence-free survival (B) of patients with LR-HCC and non-LR-HCC (Kaplan−Meier analysis). Five-year-survival rates were 91.7% (standard error [SE] 8.0) and 87.2% (SE 2.1) in LR-HCC and non-LR-HCC, respectively. The horizontal axis indicates the number of years after surgery. No significant difference in the prognosis was noted between the two groups. LR-HCC, lymphocyte rich hepatocellular carcinoma.

test. The Mann−Whitney U-test was used to examine the expression levels of CCL20 and CCR6 between LR-HCC tissues and non-LR-HCC. Multiple regression analysis was performed to search for factors related to CCL20 expression levels.

JMP Pro 16 (SAS Institute Inc., Cary, NC, USA) were used to evaluate the clinicopathological parameters and IHC results and the differences were considered statistically significant at $P < 0.05$.

3. Results

3.1. Clinicopathological features of patients with LR-HCC or non-LR-HCC

Over a 10-year period, LR-HCC was diagnosed in 28 of 451 HCC cases, with a frequency of 6.2%. Table 1 shows the clinicopathological background of 28 and 423 patients with LR-HCC and non-LR-HCC, respectively.

As for the gross type, the simple nodular type was more common in LR-HCC than in non-LR-HCC ($P = 0.0037$). However, no other significant differences were observed between LR-HCC and non-LR-HCC groups in terms of other clinical data (age, sex) and pathological data (tumor size, tissue type). Portal vein invasion, intrahepatic metastasis, and recurrence rates tended to be low in LR-HCC, but none of these trends reached statistical significance ($P = 0.5469$, $P = 0.1076$, and $P = 0.0714$, respectively).

Median follow-up was 43.3 months (IQR: 19.6−70.3 months). The K-M curves of OS and RFS are shown in Fig. 1. OS showed a 5-year survival rate of 91.7% (standard error [SE] 8.0) and 87.2% (SE 2.1) for LR-HCC and non-LR-HCC, respectively. Specifically, survival rates were better for the former cancer type, and a LR-HCC showed a tendency for improved RFS, although the difference was not statistically significant ($P = 0.4637$, $P = 0.0956$, respectively).

Histopathological characteristics of the dead and recurrent cases of LR-HCC were reviewed, but no noteworthy findings were found (data not shown).

3.2. Gene expression microarrays

We compared the cancerous and non-cancerous tissues of four LR-HCC cases using microarray analysis and extracted molecular targets with increased or decreased expression levels (Fig. 2). No factors exhibited consistently high or low expression across all four cases. However, ATG16L1, SEC24A, PPP1R3A, CCL20, and others

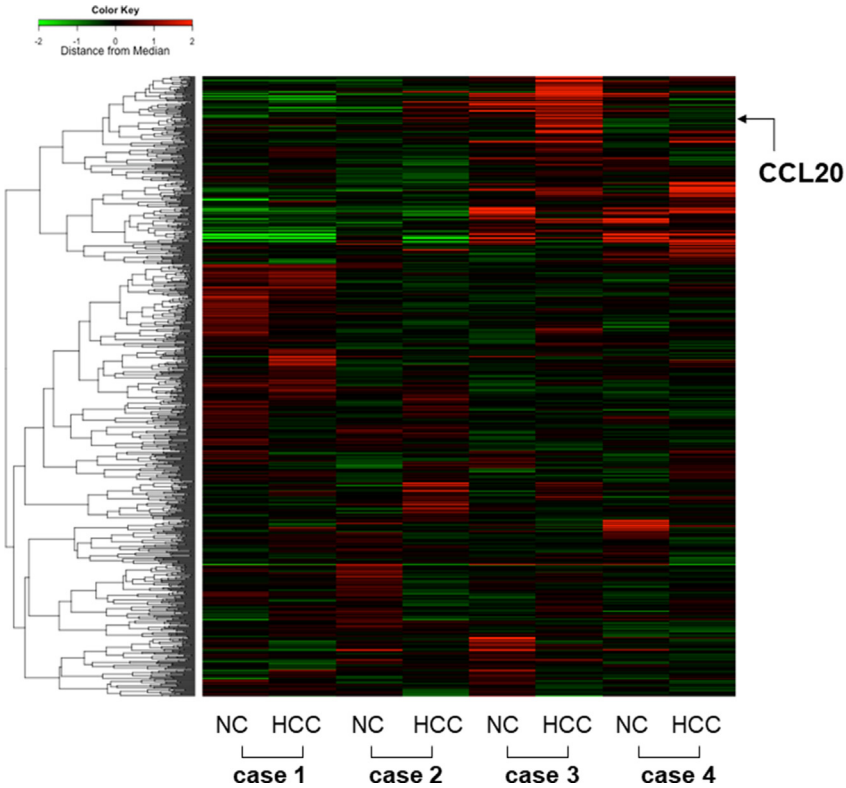

Fig. 2 Heat map focusing on chemokines based on microarray analyses of LR-HCC tissues (n = 4). Molecular targets with different levels of expression in LR-HCC tissue and its adjacent non-cancerous tissue (NC), were identified by microarray analysis. No genes were commonly elevated in the four cases, but some, including CCL20, were commonly elevated in three cases. Arrow indicates CCL20 expression. LR-HCC, lymphocyte rich hepatocellular carcinoma; CCL20, CC motif chemokine ligand (CCL) 20.

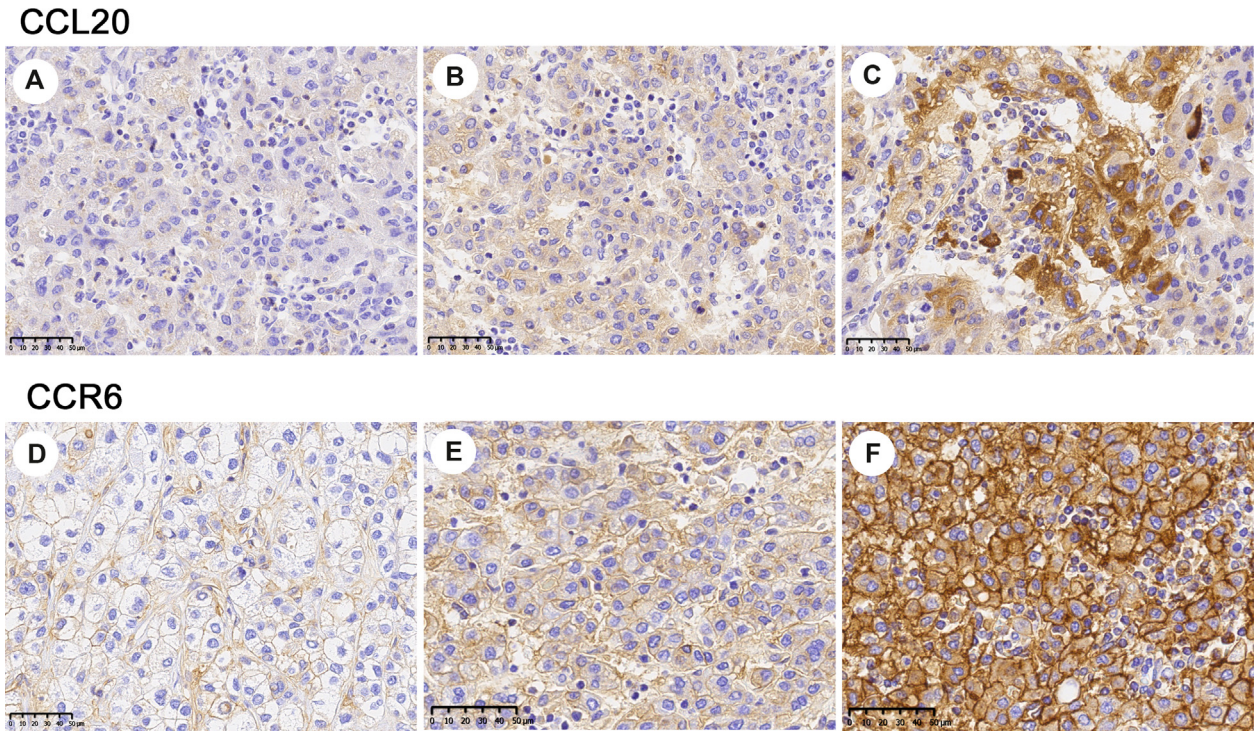

Fig. 3 Representative images of CCL20 (A, B, and C) and CCR6 (D, E, and F) expression by immunohistochemical staining. The staining intensities shown in panels A to C and in D to F were scored as 1 to 3, respectively. CCL20, CC motif chemokine ligand 20; CCR6, CC motif chemokine receptor 6.

demonstrated high expression in three out of the four cases examined. We focused on CCL20, a chemokine associated with lymphocyte infiltration.

3.3. Immunohistochemistry

Figure 3 shows the staining intensity images of CCL20 and CCR6; Fig. 4 shows the results of CCL20 staining. CCL20 expression was confirmed in tumor cells in 26 of the 28 LR-HCC cases (93%) and in 26 of 30 non-LR-HCC cases (87%). The CCL20 immunostaining score (MS) was calculated and compared in these two groups (n = 58). The mean (± standard deviation [SD]) in the LR-HCC and non-LR-HCC group was 0.62 ± 0.40 and 0.28 ± 0.31, respectively. The former was significantly higher ($P = 0.0007$) (Fig. 4E).

Figure 5 shows the staining results for CCR6, whose expression was confirmed in tumor cells in all 28 cases of LR-HCC (100%) and in 29 of 30 (97%) cases of non-LR-HCC. MS was 0.83 ± 0.43 and 0.36 ± 0.26, respectively; the former was significantly higher ($P < 0.0001$) (Fig. 5E). In addition, tumor-infiltrating lymphocytes were positive for CCR6 (Fig. 5B inset).

Regarding tumor-infiltrating lymphocytes, Fig. 6 shows H&E staining (A), CD3 staining (B), CD20 staining (C), and CD8 staining (D) results in a representative case of LR-HCC. In the 28 LR-HCC cases, the number of positive cells (mean ± SD/10HPFs) was as follows: CD3 positive, 144.0 ± 62.8; CD20 positive, 62.8 ± 43.0; and CD8 positive, 95.3 ± 43.5. Significantly more CD3-positive cells were observed compared to CD20-positive cells (Fig. 6E). In addition, the number of CD8-positive cells accounted for more than half of that of CD3-positive cells. Therefore, it can be inferred that the majority of infiltrating lymphocytes in LR-HCC were CD8-positive T cells.

3.4. Statistical analysis

Multiple regression analysis was performed using the CCL20 score obtained in both groups of LR-HCC and non-LR-HCC cases (n = 58). However, no clinicopathological factors were associated with the score. In addition, an ROC curve was created based on the results, with an AUC, CCL20 score cut-off value, sensitivity, and specificity of 0.7583, 0.25, 85.7%, and 60%, respectively. With a cutoff of 0.25, the subjects were divided into two groups of CCL20 high/low, and logistic regression analysis was performed. We examined the association with clinicopathological factors including prognosis but did not identify factors with statistically significant differences.

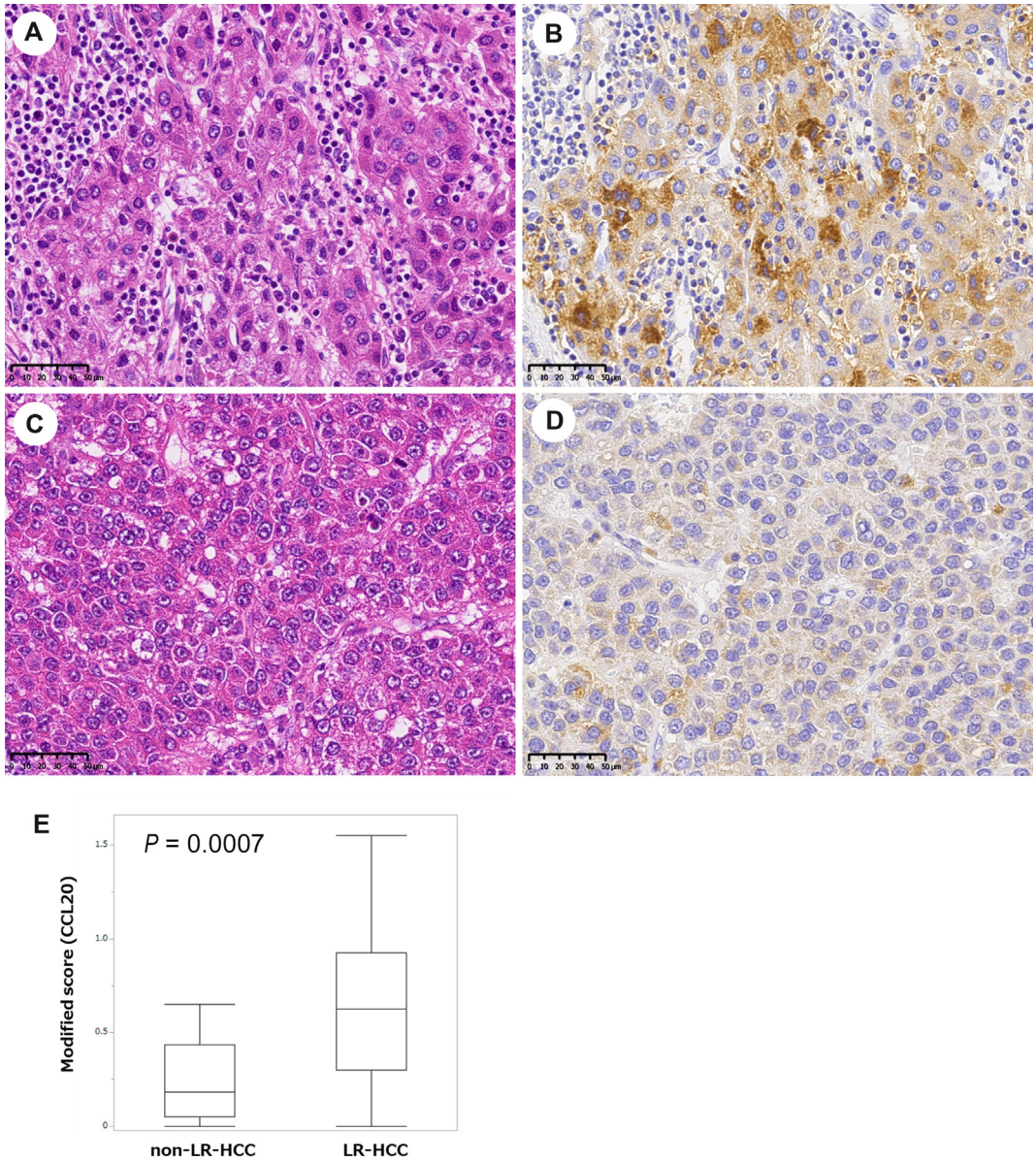

Fig. 4 A: Representative photomicrograph of an LR-HCC case (H&E). Lymphocytes outnumber tumor cells. B: CCL20 immunostaining of the same case shows a positive reaction in the tumor cells. Modified score (MS) of this case was calculated to be 1.05. C: Representative case of a non-LR-HCC showing few tumor-infiltrating lymphocytes (H&E). D: CCL20 immunostaining of non-LR-HCC shows a weakly positive to negative reaction in the tumor cells (MS = 0.15). E: CCL20 MS of LR-HCC cases was significantly higher than that of non-LR-HCC cases ($P = 0.0007$). The box represents the interquartile range. LR-HCC, lymphocyte rich hepatocellular carcinoma; H&E staining, hematoxylin-eosin staining; CCL20, CC motif chemokine ligand 20.

4. Discussion

LR-HCC is a newly proposed subtype of HCC with a relatively good prognosis. In this study, we retrospectively examined HCC cases that were surgically resected at our institution. Of the 451 HCC cases studied over a 10-year period, LR-HCC occurred in 28 cases (6.2%), which is higher than the frequency of 1% indicated by WHO. A wide range of incidence of LR-HCC has been reported previously. For example, one study reported that 216 HCCs (39.7%) showed "significant lymphocytic infiltration" in the tumor out of 544 HCC resected cases [24]. Unfortunately, there are no clear diagnostic criteria based on quantitative evaluation. This indicates the presence of differences between observers and between facilities in the criteria and accuracy of diagnosis, resulting in variations in frequency.

In this study, we compared the clinicopathological factors of LR-HCC and non-LR-HCC cases. No statistically significant differences were observed in the factors, except

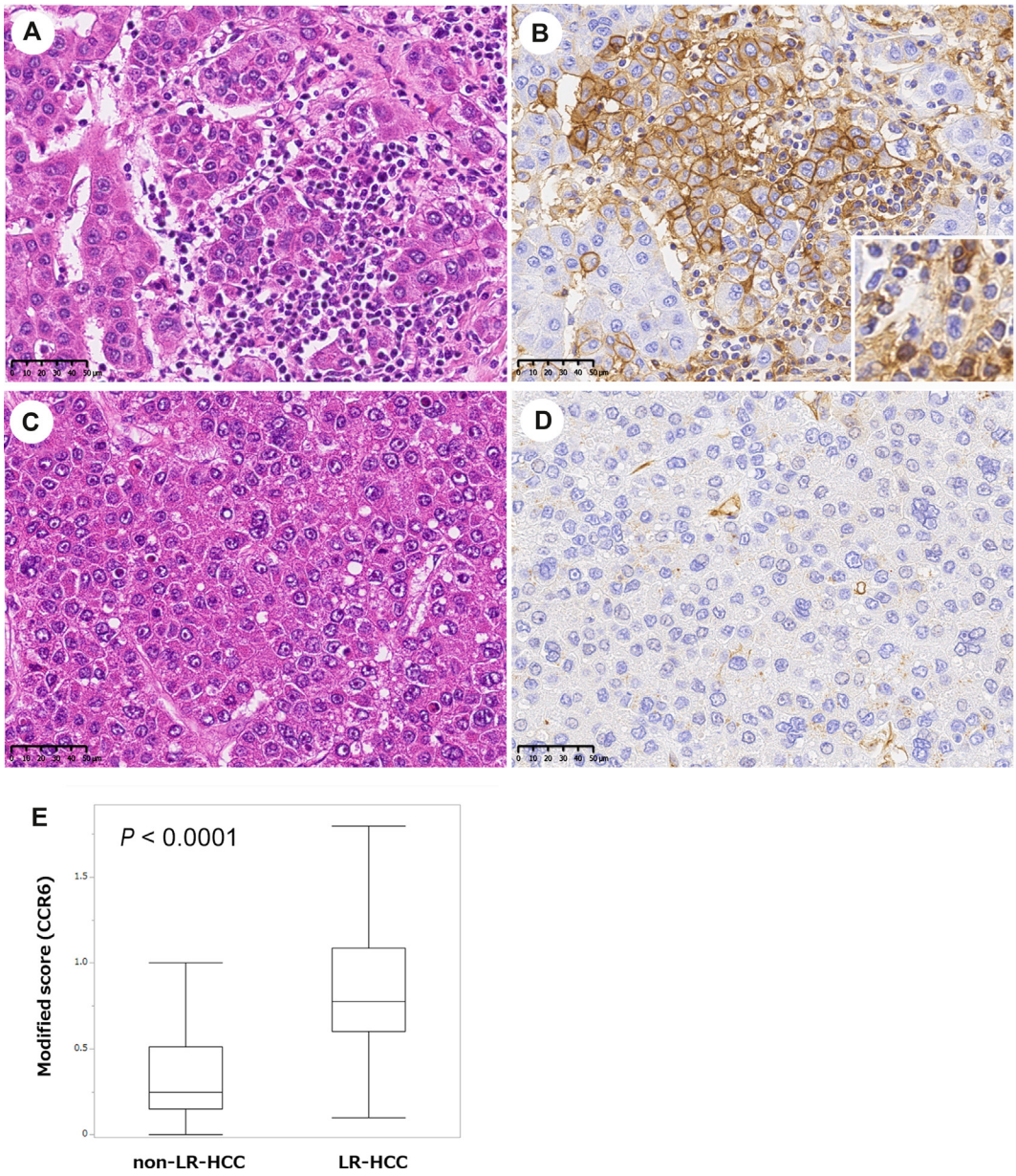

Fig. 5 A: Representative photomicrograph of an LR-HCC case (H&E). B: CCR6 immunostaining of an LR-HCC case shows a positive reaction in the tumor cells with a Modified score (MS) of 0.55. CCR6 expression is also noted in tumor-infiltrating lymphocytes (inset). C: Representative case of a non-LR-HCC (H&E). D: A non-LR-HCC shows few CCR6 positive cells with a MS of 0.1. E: CCR6 MS of LR-HCC cases was significantly higher than that of non-LR-HCC cases ($P < 0.0001$). The box represents the interquartile range. LR-HCC, lymphocyte rich hepatocellular carcinoma; H&E staining, hematoxylin-eosin staining; CCR6, CC motif chemokine receptor 6.

for gross type, although intrahepatic metastasis and recurrence rates tended to be low in LR-HCC. Regarding prognosis, no significant difference was observed between LR-HCC and non-LR-HCC. However, a previous report from our institution showed that the 5-year survival rate for all HCC resected cases was 65% [6], which was approximately 80% in the present study, suggesting that the prognosis of resected HCC cases in our institution has improved dramatically in the 30 years since the previous study. In general, the 5-year survival rate after surgery for HCC is often reported to be 20−57% [25] and was estimated to be 65% for Child−Pugh A cases in Japan [26]. In the present study, it is conceivable that the survival rate of the included cases was high, and consequently, we were unable to achieve a statistically significant difference. Nevertheless, the 5-year survival rate for LR-HCC at our institution exceeded 90%. Therefore, the prognosis of LR-HCC can be concluded to be good.

In this study, we performed a comprehensive microarray analysis and found CCL20 to be highly expressed in LR-

HCC. CCL20 is a chemokine involved in lymphocyte migration, with CCR6 as its sole receptor [27]. We investigated CCL20 expression in actual tumor tissues and found that it was higher in the LR-HCC group than that in the non-LR-HCC group. In addition, CCR6 expression was confirmed in lymphocytes within the tumor tissue, suggesting that CCL20 may be involved in the migration of intratumoral lymphocytes. Furthermore, CCR6 is highly expressed in the tumor cells, suggesting that CCL20 may act in an autocrine manner.

CCL20, also known as liver and activation-regulated chemokine (LARC) and was originally found in the liver [28]. It is involved in inflammation and has been implicated in inflammatory and infectious diseases, such as rheumatoid arthritis and human immunodeficiency virus infection. In addition, the axis between CCL20 and its receptor, CCR6, may be involved in the chemotaxis of T cells, B cells, and dendritic cells (DC). This axis has also been implicated in the recruitment of immature DCs to sites of antigen entry and the arrest of T lymphocytes on the

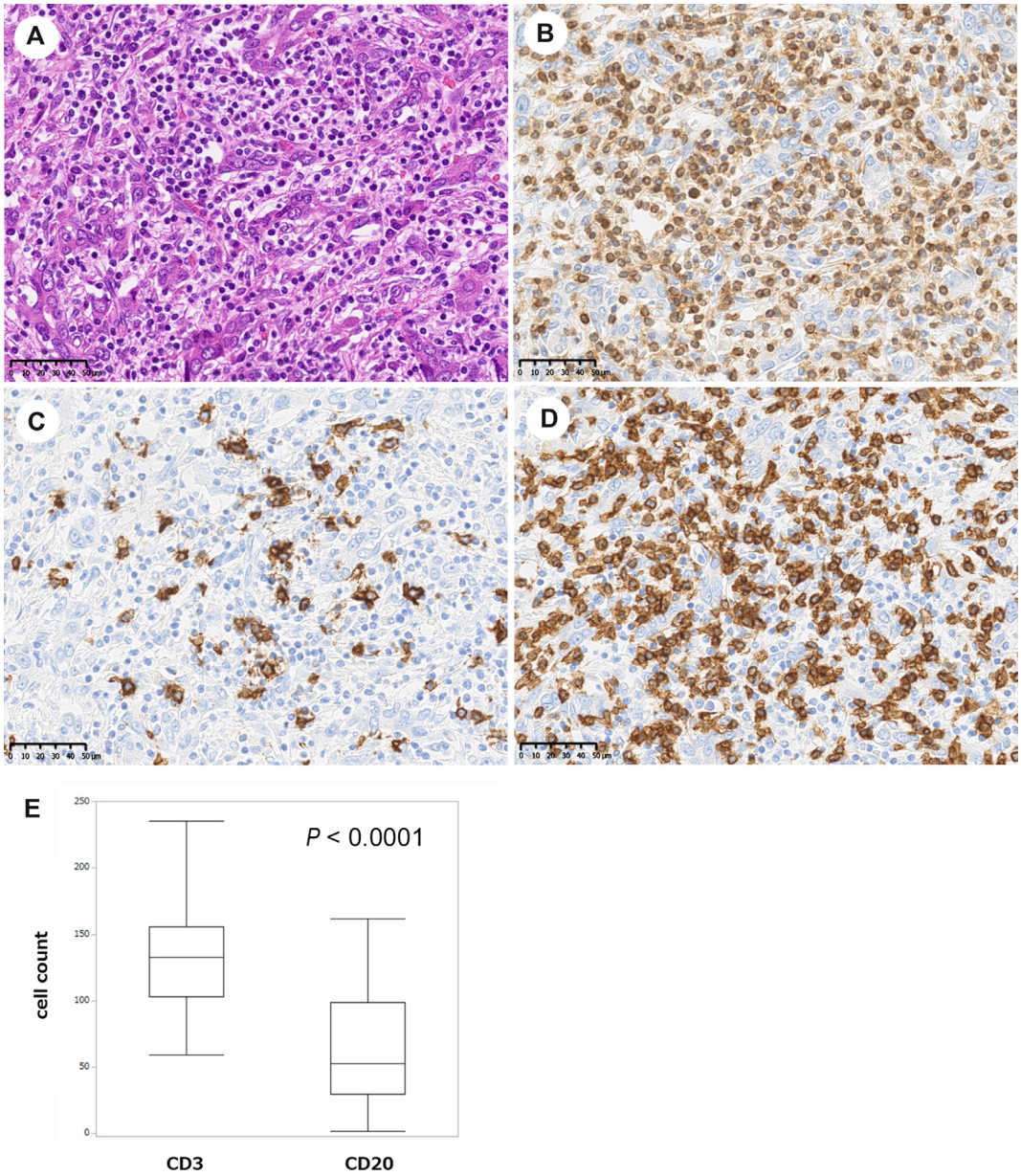

Fig. 6 A: Representative photomicrograph of an LR-HCC case (H&E). B−D: IHC staining results of CD3 (B), CD20 (C) and CD8 (D). Intra-tumor infiltrating lymphocytes show more CD3-positive cells than CD20, and the number of CD8-positive cells accounted for more than half of that of CD3-positive cells. E: Comparison of the number of positive cells between CD3 and CD20 in LR-HCCs (n = 28) revealed a significantly higher number in the former ($P < 0.0001$). The vertical axis shows the average number of lymphocytes in 10 high-magnification fields of view. LR-HCC, lymphocyte rich hepatocellular carcinoma; H&E staining, hematoxylin-eosin staining.

endothelium during the early stages of the immune response and has recently been implicated in intratumoral immunity.

Since the 2010s, the development of immune checkpoint inhibitor-based therapies has led to progress in research on how tumors evade immune detection, which decreases the effectiveness of immune checkpoint inhibitors. In HCC, WNT/β-catenin mutations may induce immune evasion, and CCL20 is involved in this mechanism. Studies using mouse HCC models and human HCC samples have shown that several chemokines, including CCL20, are downregulated in HCC with WNT/β-catenin mutations. Furthermore, the mutation reduces the infiltration of CD8-positive T cells into tumor tissues, suggesting the involvement of CCL20 with CD8-positive T cells [29]. Akasu M et al. showed that β-catenin-activated HCC cell lines overexpressing cytokines, including CCL20, restores the cell-killing ability of T lymphocytes [30]. In addition, although the organ is different, that high CCL20 and CD8-positive cell counts were observed to be associated with COVID-19 alveoli, and that they were involved in the persistence of inflammation [31]. The infiltrating lymphocytes in the LR-HCC tumors examined in this study were predominantly CD8-positive T cells, and this is consistent with previous reports that CCL20 contributes to the increase of CD8-positive T cells.

To confirm the β-catenin mutation, immunostaining in the LR-HCC cases revealed its positivity (with nuclear staining) in only two of 28 cases (7.1%) (data not shown). These mutations reportedly have been identified in upto 40% of resected HCCs [32], and are clearly less common in LR-HCC cases, consistent with reports of correlation between β-catenin mutations and CCL20 suppression.

CCL20 has a tumor-promoting effect in multiple tumor types, including HCC. This effect is mediated by the autocrine action of CCL20 via CCR6 [33]. CCL20 also recruits regulatory T cells via CCR6, which can suppress tumor immunity [34,35]. However, these studies are likely to have been conducted on conventional HCC, and it is possible that LR-HCC, which was targeted in the present study, was not included due to its low frequency. In our study, the infiltrating lymphocytes were mainly CD8-positive lymphocytes. Specifically, in LR-HCC, CCL20 recruits cytotoxic CD8-positive lymphocytes through CCR6, rather than autocrine tumor growth-promoting action. This improves the tumor immune microenvironment and yields antitumor effects. This may be the reason for the relatively favorable prognosis.

This study had some limitations. Our results suggest that CCL20 may be involved in lymphocyte migration in LR-HCC tumors. However, due to the overall rarity of LR-HCC, the number of cases examined was small (n = 28), which may not be sufficient as a sample size. Nonetheless, over the past 10 years, we have examined a population of just under 500 cases; thus, we believe that this was a reasonably large cohort. In addition, although CCR6 expression was confirmed in tumor-infiltrating lymphocytes, it was not confirmed whether this expression was consistent with CD8-positive cells. We will continue to accumulate cases and examine the clinicopathological characteristics of LR-HCC

5. Conclusions

In this study, we examined LR-HCC cases at our institution and found that the frequency of incidence was 6.2%, which is higher than previous reports. There were no statistically significant differences in clinicopathological factors between LR-HCC and non-LR-HCC, except for gross type, although intrahepatic metastasis and recurrence rates tended to be low in LR-HCC and the 5-year survival rate for LR-HCC was well over 90%. Infiltrating lymphocytes in the tumor stroma of LR-HCC were mainly composed of CD8-positive T cells. CCL20 expression was significantly higher in LR-HCC than that in non-LR-HCC, suggesting that CCL20 may be involved in intratumoral lymphocyte migration.

Acknowledgments

The authors would like to thank Akiko Tanaka, Sachiyo Maeda and Akemi Fujiyoshi for their technical assistance and Dr. Kaori Yasuda and Dr. Hiroko Hagiwara (Cell Innovator, Fukuoka, Japan) for assistance with the RNA array analyses and for useful advice and discussions. We would also like to thank Editage (www.editage.com) for English language editing.

Author contributions: K.T., M.N., S.O., J.A., and H.Y. conceptualized and designed this study. K.T., M.N., R.K., Y.M., Y.Y., S.M., Y.K., and J.A. conducted the study. K.T., M.N., and S.O. managed and analyzed the data. K.M. was in charge of statistical analysis. K.T. and S.O. prepared the manuscript. The manuscript was reviewed and revised by J.A. and H.Y., and the final version was approved for submission by all authors.

Disclosures: None.

Funding: This research did not receive any specific grant from funding agencies in the public, commercial, or not-for-profit sectors.

References

[1] Torbenson MS, Ng IOL, Park YN. Hepatocellular carcinoma. In: Paradis V, Fukayama M, Park YN, Schirmacher P, editors. WHO classification of tumours of the digestive system. 5th ed. Lyon, France: IRAC Press; 2019. p. 229–39.

[2] Kudo M, Finn RS, Qin S, et al. Lenvatinib versus sorafenib in first-line treatment of patients with unresectable hepatocellular carcinoma: a randomised phase 3 non-inferiority trial. Lancet 2018;391:1163–73. https://doi.org/10.1016/S0140-6736(18)30207-1.

[3] Sung H, Ferlay J, Siegel RL, et al. Global cancer statistics 2020: GLOBOCAN estimates of incidence and mortality worldwide for 36 cancers in 185 countries. CA Cancer J Clin 2021;71:209−49. https://doi.org/10.3322/caac.21660.
[4] Chan AW, Tong JH, Pan Y, et al. Lymphoepithelioma-like hepatocellular carcinoma: an uncommon variant of hepatocellular carcinoma with favorable outcome. Am J Surg Pathol 2015;39:304−12. https://doi.org/10.1097/PAS.0000000000000376.
[5] Labgaa I, Stueck A, Ward SC. Lymphoepithelioma-like carcinoma in liver. Am J Pathol 2017;187:1438−44. https://doi.org/10.1016/j.ajpath.2017.02.022.
[6] Wada Y, Nakashima O, Kutami R, Yamamoto O, Kojiro M. Clinicopathological study on hepatocellular carcinoma with lymphocytic infiltration. Hepatology 1998;27:407−14. https://doi.org/10.1002/hep.510270214.
[7] Emile JF, Adam R, Sebagh M, et al. Hepatocellular carcinoma with lymphoid stroma: a tumour with good prognosis after liver transplantation. Histopathology 2000;37:523−9. https://doi.org/10.1046/j.1365-2559.2000.00952.x.
[8] Eun S, Jeon YK, Jang JJ. Hepatocellular carcinoma with immature T-cell (T-lymphoblastic) proliferation. J Kor Med Sci 2010;25:309−12. https://doi.org/10.3346/jkms.2010.25.2.309.
[9] Patel KR, Liu TC, Vaccharajani N, Chapman WC, Brunt EM. Characterization of inflammatory (lymphoepithelioma-like) hepatocellular carcinoma: a study of 8 cases. Arch Pathol Lab Med 2014;138:1193−202. https://doi.org/10.5858/arpa.2013-0371-OA.
[10] Yuan L, Aucejo F, Menon KVN, Liu X. Lymphoepithelioma-like hepatocellular carcinoma: report of three cases and review of literature. J Med Cases 2015;6:297−303. https://doi.org/10.14740/jmc2106w.
[11] Wang JK, Jin YW, Hu HJ, et al. Lymphoepithelioma-like hepatocellular carcinoma: a case report and brief review of literature. Medicine 2017;96:e9416. https://doi.org/10.1097/MD.0000000000009416.
[12] Miyasaka C, Ishida M, Ito H, Kaibori M, Uemura Y, Tsuta K. Lymphoepithelioma-like hepatocellular carcinoma: a case report with emphasis on the cytological features. Int J Clin Exp Pathol 2017;10:7893−7.
[13] Filotico M, Moretti V, Floccari F, D'Amuri A. Very rare liver neoplasm: lymphoepithelioma-like (LEL) hepatocellular carcinoma. Case Rep Pathol 2018;2018:2651716. https://doi.org/10.1155/2018/2651716.
[14] Shih EJ, Chau IY, Yeh YC, Chau GY. Synchronous hepatocellular carcinoma and lymphoepithelioma-like carcinoma arising from 2 different sites of the liver: a case report. Medicine 2018;97:e12548. https://doi.org/10.1097/MD.0000000000012548.
[15] Zhang K, Tao C, Tao Z, et al. Lymphoepithelioma-like carcinoma in liver not associated with Epstein-Barr virus: a report of 3 cases and literature review. Diagn Pathol 2020;15:115. https://doi.org/10.1186/s13000-020-01035-6.
[16] Iwasaki T, Kubota A, Suzuki M, Terada T. A case of small well-differentiated hepatocellular carcinoma with marked lymphocytic infiltrate. Int J Clin Exp Pathol 2020;13:624−33.
[17] Noguchi H, Noguchi N, Idichi T, et al. Case report of a lymphoepithelioma-like hepatocellular carcinoma with prominent lymphoplasmacytic infiltration. Hum Pathol Case Rep 2020;21:200402. https://doi.org/10.1016/j.ehpc.2020.200402.
[18] Raab-Traub N. Epstein-Barr virus in the pathogenesis of NPC. Semin Cancer Biol 2002;12:431−41. https://doi.org/10.1016/s1044579x0200086x.
[19] Chen B, Zhang Y, Dai S, et al. Molecular characteristics of primary pulmonary lymphoepithelioma-like carcinoma based on integrated genomic analyses. Signal Transduct Targeted Ther 2021;6:6. https://doi.org/10.1038/s41392-020-00382-6.
[20] Ohtani H, Jin Z, Takegawa S, Nakayama T, Yoshie O. Abundant expression of CXCL9 (MIG) by stromal cells that include dendritic cells and accumulation of CXCR3+ T cells in lymphocyte-rich gastric carcinoma. J Pathol 2009;217:21−31. https://doi.org/10.1002/path.2448.
[21] Cancer Genome Atlas Research Network, Electronic address: wheeler@bcm.edu, Cancer Genome Atlas Research Network. Comprehensive and integrative genomic characterization of hepatocellular carcinoma. Cell 2017;169:1327−1341.e23.
[22] Quackenbush J. Microarray data normalization and transformation. Nat Genet 2002;32:496−501. https://doi.org/10.1038/ng1032.
[23] Umeno Y, Ogasawara S, Akiba J, et al. Regulator of G-protein signaling 5 enhances portal vein invasion in hepatocellular carcinoma. Oncol Lett 2018;15:1763−70. https://doi.org/10.3892/ol.2017.7474.
[24] Hayashi A, Shibahara J, Misumi K, et al. Histologic assessment of intratumoral lymphoplasmacytic infiltration is useful in predicting prognosis of patients with hepatocellular carcinoma. PLoS One 2016;11:e0155744. https://doi.org/10.1371/journal.pone.0155744.
[25] Lee JG, Kang CM, Park JS, et al. The actual five-year survival rate of hepatocellular carcinoma patients after curative resection. Yonsei Med J 2006;47:105−12. https://doi.org/10.3349/ymj.2006.47.1.105.
[26] Kudo M. Surveillance, diagnosis, and treatment outcomes of hepatocellular carcinoma in Japan: 2021 update. Liver Cancer 2021;10:167−80. https://doi.org/10.1159/000516491.
[27] Baba M, Imai T, Nishimura M, et al. Identification of CCR6, the specific receptor for a novel lymphocyte-directed CC chemokine LARC. J Biol Chem 1997;272:14893−8. https://doi.org/10.1074/jbc.272.23.14893.
[28] Schutyser E, Struyf S, Van Damme J. The CC chemokine CCL20 and its receptor CCR6. Cytokine Growth Factor Rev 2003;14:409−26. https://doi.org/10.1016/s1359-6101(03)00049-2.
[29] Ruiz de Galarreta M, Bresnahan E, Molina-Sánchez P, et al. β-Catenin activation promotes immune escape and resistance to anti-PD-1 therapy in hepatocellular carcinoma. Cancer Discov 2019;9:1124−41. https://doi.org/10.1158/2159-8290.CD-19-0074.
[30] Akasu M, Shimada S, Kabashima A, et al. Intrinsic activation of β-catenin signaling by CRISPR/Cas9-mediated exon skipping contributes to immune evasion in hepatocellular carcinoma. Sci Rep 2021;11:ID16732. https://doi.org/10.1038/s41598-021-96167-0.
[31] Saris A, Reijnders TDY, Reijm M, et al. Enrichment of CCR6+ CD8+ T cells and CCL20 in the lungs of mechanically ventilated patients with COVID-19. Eur J Immunol 2021;51:1535−8. https://doi.org/10.1002/eji.202049046.
[32] Calderaro J, Couchy G, Imbeaud S, et al. Histological subtypes of hepatocellular carcinoma are related to gene mutations and molecular tumour classification. J Hepatol 2017;67:727−38. https://doi.org/10.1016/j.jhep.2017.05.014.
[33] Kadomoto S, Izumi K, Mizokami A. The CCL20-CCR6 axis in cancer progression. Int J Mol Sci 2020;21. https://doi.org/10.3390/ijms21155186.
[34] Rutihinda C, Haroun R, Saidi NE, et al. Inhibition of the CCR6-CCL20 axis prevents regulatory T cell recruitment and sensitizes head and neck squamous cell carcinoma to radiation therapy. Cancer Immunol Immunother 2023;72:1089−102. https://doi.org/10.1007/s00262-022-03313-2.
[35] Wang D, Yang L, Yu W, et al. Colorectal cancer cell-derived CCL20 recruits regulatory T cells to promote chemoresistance via FOXO1/CEBPB/NF-κB signaling. J Immunother Cancer 2019;7:215. https://doi.org/10.1186/s40425-019-0701-2.